Effects of Pyridine Exposure upon Structural Lipid Metabolism in Swiss Webster Mice

ARTICLE *in* CHEMICAL RESEARCH IN TOXICOLOGY · APRIL 2008

Impact Factor: 3.53 · DOI: 10.1021/tx7002454 · Source: PubMed

5 AUTHORS, INCLUDING:

Craig E Wheelock
Karolinska Institutet
111 PUBLICATIONS **2,061** CITATIONS
SEE PROFILE

Jenny Forshed
Karolinska Institutet
29 PUBLICATIONS **502** CITATIONS
SEE PROFILE

Susumu Goto
Kyoto University
172 PUBLICATIONS **22,776** CITATIONS
SEE PROFILE

John William Newman
United States Department of Agriculture
133 PUBLICATIONS **4,720** CITATIONS
SEE PROFILE

Effects of Pyridine Exposure upon Structural Lipid Metabolism in Swiss Webster Mice

Craig E. Wheelock,*[,†,‡,§] Jenny Forshed,[||] Susumu Goto,[§] Bruce D. Hammock,*[,†] and John W. Newman[†,⊥]

Department of Entomology and Cancer Research Center, University of California, Davis, California 95616, Division of Physiological Chemistry II, Department of Medical Biochemistry and Biophysics, Karolinska Institutet, Scheeles väg 2, SE-171 77 Stockholm, Sweden, Bioinformatics Center, Institute for Chemical Research, Kyoto University, Kyoto 611-0011, Japan, and Karolinska Biomics Center, Karolinska University Hospital Solna, Z5:02, 17176, Stockholm, Sweden

Received July 9, 2007

Pyridine is a prototypical inducer of cytochrome P450 (CYP) 2E1, an enzyme associated with cellular oxidative stress and membrane damage. To better understand the effect of this treatment on cellular lipids, the influence of pyridine exposure (100 mg/kg/day i.p. for 5 days) on fatty acids, fatty esters, and fatty alcohol ethers in brain, heart, liver, and adipose tissue from male Swiss Webster mice was investigated. Lipid levels in cholesterol esters, triglycerides, free fatty acids, cardiolipin, sphingomyelin, and glycerylphospholipids were quantified. Pyridine altered the level and composition of lipids involved in membrane structure (i.e., sphingomyelin, phosphatidylethanolamines, and plasmalogens), energy metabolism (i.e., free fatty acids), and long-chain fatty acid transport (i.e., cholesterol esters) in a tissue-specific manner. Subtle changes in cholesterol esters were observed in all tissues. Sphingomyelin in the brain and heart were depleted in monounsaturated fatty acids (1.4- and 1.5-fold, respectively), while the liver sphingomyelin concentrations increased (1.5-fold). Pyridine exposure also increased heart free fatty acids by 1.3-fold, enriched cardiac phosphatidylethanolamine in long-chain polyunsaturated fatty acids by 1.3-fold, and depleted cardiolipin-associated plasmalogens by 3.8-fold. Phosphatidylethanolamines in the brain were also enriched in both saturated fatty acids (1.2-fold) and polyunsaturated fatty acids (1.3-fold) but were depleted in plasmalogens (2.9-fold). In particular, the levels of phosphatidylethanolamine-associated arachidonic (AA) and docosahexaenoic acid (DHA) in both brain and cardiac tissues significantly decreased following pyridine exposure. Considering the hypothetical role of plasmalogens as membrane-bound reactive oxygen scavengers, the current findings suggest that the brain and heart should be the focus of future studies on the toxicity of pyridine, as well as other CYP 2E1 inducers.

Introduction

Pyridine (azabenzene or azine) is a simple heterocyclic aromatic compound obtained from coal tar, with ~50% of the manufactured pyridine being used in the production of agricultural chemicals and other industrial agents including pharmaceuticals, disinfectants, and vitamins (*1*). Moreover, pyridine is found in several naturally occurring products, appearing at trace levels in food and in byproducts of combustion, including tobacco smoke (*1, 2*). Pyridine is a nongenotoxic carcinogen, with chronic exposure to high levels (i.e., ≥250 ppm) in water producing hepatocellular neoplasms in rats and mice (*3*). Shorter exposures to moderate doses (i.e., ~200 mg/kg) produce hepatomegaly without chemical-related lesions (*3*). Regardless, a number of deleterious health effects have been associated with pyridine exposure, including damage to the central nervous system, liver, and kidneys as well as gastrointestinal upset (*1, 4*). Symptoms of neurotoxicity are the most evident from acute exposures (*4*), manifesting as headaches, nausea, vomiting, dizziness, and nervousness in humans (*1*). These sublethal effects of pyridine exposure and the biochemical alterations behind them are poorly understood.

Acute pyridine exposure induces a number of cytochrome P450 (CYP)[1] isozymes including 1A1, 1A2, 2B1, 2B2, 4B, and 2E1 (*5, 6*); however, it is especially effective at increasing levels of the ethanol-inducible isozyme CYP 2E1 in rodents (*5, 7*). This enzyme is also induced in humans with perturbations of liver function apparently associated with fatty liver (*8*). The activation of CYP 2E1 results in increased production of reactive oxygen species (ROS), such as superoxide and hydrogen peroxide (*9*), which can oxidize lipids resulting in membrane damage (*10, 11*) and loss of membrane integrity (*12, 13*). Furthermore, CYP 2E1-linked oxidative stress activates cyclooxygenase-2 expression in vivo (*14*), consistent with an

* To whom correspondence should be addressed. (B.D.H.) Tel: 530-752-8465. Fax: 530-752-1537. E-mail: bdhammock@ucdavis.edu. (C.E.W.) Tel: +46 8 5248-7630. Fax: +46 8 763-0439. E-mail: craig.wheelock@ki.se.
† University of California.
‡ Karolinska Institutet.
§ Kyoto University.
|| Karolinska University Hospital Solna.
⊥ Current address: Western Human Nutrition Research Center, Agricultural Research Service, U.S. Department of Agriculture, and Department of Nutrition, University of California Davis, Davis, CA 95616.

[1] Abbreviations: AA, arachidonic acid; CE, cholesterol ester; CL, cardiolipin; CYP, cytochrome P450; DHA, docosahexaneoic acid; EDTA, ethylenediaminetetraacetic acid; FDR, false discovery rate; FFA, free fatty acid; LPC, lyso-phosphatidylcholine; MUFA, monounsaturated fatty acids; n3, ω 3 fatty acids; n6, ω 6 fatty acids; n7, products of the δ-9 desaturase; PC, phosphatidylcholine; PE, phosphatidylethanolamine; PLS, partial least squares; PM, plasmalogen; PS, phosphatidylserine; PUFA, polyunsaturated fatty acids; ROS; reactive oxygen species; SAT, saturated fatty acids; SM, sphingomyelin; TG, triglycerides; TPL, total phospholipids; trans, *trans*-fatty acids.

10.1021/tx7002454 CCC: $40.75
Published on Web 02/06/2008

inflammatory response. In mice, a 3 month pyridine exposure resulted in oxidative tissue damage, including increased lipid peroxidation in the liver, as well as within various regions of the brain (*15*). Accordingly, adaptive responses in lipid metabolism associated with elevated oxidative stress would be expected in tissues from pyridine-exposed organisms; however, the extent and nature of such an effect have not been examined.

This study was designed to evaluate the effect of a short-term, low-dose pyridine exposure on lipid metabolism in tissues either reported to be affected by pyridine exposure (liver and brain) or with metabolic phenotypes geared toward lipid combustion (heart) and storage (adipose). To provide a broad metabolic base for this investigation, a "lipidomics" approach was employed focusing on components likely affected by alterations in membrane integrity. The results provide novel insights into the effects of pyridine exposure on lipid metabolism.

Experimental Procedures

Animals. Male Swiss Webster mice were purchased from Charles River Breeding Laboratory (Hollister, CA) and were 20–25 g upon receipt. Mice were housed in HEPA-filtered racks for 7 days before use and were fed and watered ad libitum with a light cycle of 12 h light and 12 h dark. Animal care procedures were approved by the Animal Use and Care Committee at the University of California, Davis. Pyridine (100 mg/kg) in corn oil was injected into the intraperitoneal (i.p.) cavity daily for 5 days, and control mice were injected with an equal volume of vehicle alone as previously described (*6*). A dose of 100 mg/kg per day was chosen since this level is sufficient to induce CYP 2E1 in rodents (*7, 16*), is between 2- and 10-fold of the rat oral no observable effect level for a variety of outcomes (*1*), and is more than 10-fold lower than the murine i.p. LC_{50} value of 1200 mg/kg (*17*). On the sixth day, mice were sacrificed with a lethal dose of pentobarbital. All organs were immediately excised, rinsed in a sodium chloride solution (1% w/v), snap frozen in liquid nitrogen, and stored at −80 °C. The control results have been used as a comparative set for a similar investigation of the effects of clofibrate on lipid metabolism, which appeared in an independent report (*18*).

Lipid Analysis. Lipids were quantified by Lipomics Technologies (West Sacramento, CA; http://www.lipomics.com) as previously described (*18–21*). Briefly, tissue samples were spiked with a suite of analytical surrogates [lipid classes containing 17:0 as its fatty acid component, i.e., for cholesterol esters (CE) cholesteryl heptadecanoate was used, etc.] for each lipid class and homogenized in chloroform:methanol (2:1 v/v) in the presence of the antioxidant butylated hydroxyl toluene (0.05%). The total lipid extracts from equivalents of 25 mg of brain, heart, or liver tissue or 10 mg of inguinal adipose tissue were then separated by preparative thin-layer chromatography, and lipid classes were isolated by scraping bands marked by cochromatographed standards contained on the same plates as described by Ruiz and Ochoa (*22*). Chromatography plates were conditioned prior to use by washing with an ethylene-diaminetetraacetic acid (EDTA) solution (1 mM, pH 5.5) to remove divalent cations and pre-eluted with chloroform:methanol to eliminate background contamination. Conditioned plates were dried and stored under nitrogen prior to use, and all thin-layer separations were performed under an inert gas atmosphere. Isolated lipid classes were treated with 100 °C 3 N HCl in methanol, and the resulting fatty acid methyl esters and 1-vinylic-ether-derived dimethyl acetals were back extracted with hexane. The hexane extracts were then analyzed by gas chromatography using a 0.25 mm i.d. × 30 m 5 μm DB-225MS capillary column (J&W Scientific, Folsom, CA) and a flame ionization detector. Concentrations (nmol/g tissue) of lipids are reported for various lipid subclasses, including total fatty acids (the sum of all fatty acids analyzed), saturated fatty acids (SAT), monounsaturated fatty acids (MUFA), polyunsaturated fatty acids (PUFA), ω 3 fatty acids (n3), ω 6 fatty acids (n6), products of the δ-9 desaturase (n7 and n9), plasmalogen (PM)-linked fatty acids, and trans. Concentrations of all measured lipids are provided on a tissue-selective basis in the Supporting Information (Tables S1−S4) as well as an overview of fatty acid nomenclature (Table S5). All results are corrected for surrogate recoveries and expressed as a function of tissue wet mass.

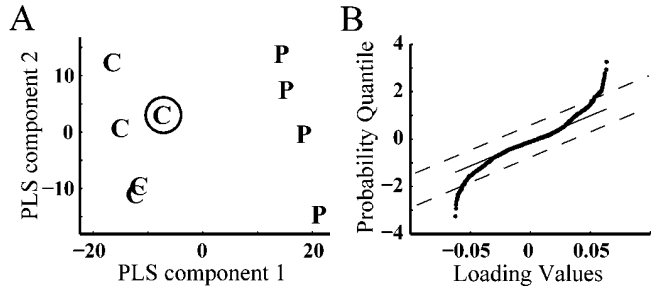

Figure 1. Representative PLS analysis results. A PLS scores plot from a representative cross-validation is shown in panel A. The circled sample was held out from the PLS modeling, and the model properly predicted its class assignment. The included variables are those selected in the PLS variable selection: "C" denotes control mice, and "P" denotes pyridine-treated mice. All variables are provided in Table S6. The normal probability plot in panel B shows each loading variable value (●). The variables exceeding the limits ±1 standard deviation (broken lines) from the mean (solid line) were selected as significantly important to the PLS model with a 68% confidence interval.

Data Analysis and Statistics. The complete data set is provided in Tables S1−S4, with nondetected values shown as blank data (no entry in the table) and measured values below the detection limit provided as "zeros". All variables with nondetected values were excluded for the purpose of performing partial least squares (PLS) analysis (a list of excluded variables is provided in Table S7). All values reported in the text are means ± standard deviations of nmol/g tissue concentrations. The PLS and Jack-knifing calculations were performed using in-house routines written with MATLAB (version 7.4).

Significance was initially assigned to differences in mean lipid concentrations between treated and control mice based on two-tailed Student's t tests ($p \leq 0.05$) for each individual lipid, with all calculated p values shown in Tables S1−S4. The changes suggested by this analysis are displayed in a heat map of differences from controls in Figure 2. Controlling for the false discovery rate (FDR) with a $q = 0.1$ by the methods of Benjamini and Hochberg (*23*), a maximum FDR-adjusted p value of 0.00686 was identified when the entire data set of 1077 valid hypotheses was tested. This analysis reduced the total number of significant changes to 72.

The data set was further analyzed using a multivariate PLS model, which identifies the combination of variables that best describe group differences (*24*). These results were cross-validated, and the resulting significant variables were ranked by Jack-knifing (*25*). Using leave-one-out cross-validation, nine models were created where one animal at a time was held out of the modeling and then predicted (Figure 1A). The created models were analyzed in terms of which lipids drove the separation of pyridine-treated and control mice. This analysis was performed by studying the loading variables from each PLS model. Loading variables exceeding ±1 standard deviation of the loading distribution, that is, larger than noise, were noted as influential to the PLS model and hence important to the observed class separation. Results were visualized by a normal probability plot showing samples deviating from a normal distribution (Figure 1B).

The selected variables were then ranked by Jack-knifing. At each cross-validation, the first loading vector p, describing the discriminating variables, was selected. The variability of influence of the different variables was then estimated by comparing the loading vectors from all the cross-validation models. The standard deviation for each variable k was estimated by:

$$sp_k = \sqrt{\sum_{m=1}^{M} \{(p_k - p_{km})\sqrt{[(M-1)/M]}\}^2}$$

where M = the number of cross-validations (nine in this case), m = the specific cross-validation occasion, and p_k = the loading value at variable k. The variables were then ranked so that the component with the highest loading (mean) and the smallest standard deviation received the highest rank (Table S6).

The numbers of identified variables, along with their vector, tissue, and lipid class distributions, are shown in Figure 3 and compare well with metabolites affected by pyridine treatment identified using the FDR-adjusted p values (Figure S1). Table S6 shows all identified metabolites for distinguishing pyridine treatment vs control. The Student's two-tailed t test identified 83 variables with p values <0.01, and the PLS model identified 75 variables (at the 68% confidence interval), of which 68 agreed with the t test analysis. The FDR adjustment reduced the number of significant variables from 83 to 72 at the $p < 0.01$ level, of which the PLS and FDR-adjusted analyses had 60 in common. To provide a general overview of observed fluctuations in lipid levels, data presented in the Results are reported as "significant" based upon the Student's t test ($p < 0.05$), which correspond to the changes displayed in Figure 2. From this data set, those lipids that were identified to be significant by both the PLS and the FDR-adjusted p value models (Table S6), representing our highest level of confidence, are then further examined in the Discussion.

Results

Brain Lipid Metabolism. Pyridine exposure produced clear changes in brain lipids, due mainly to shifts in phospholipid,

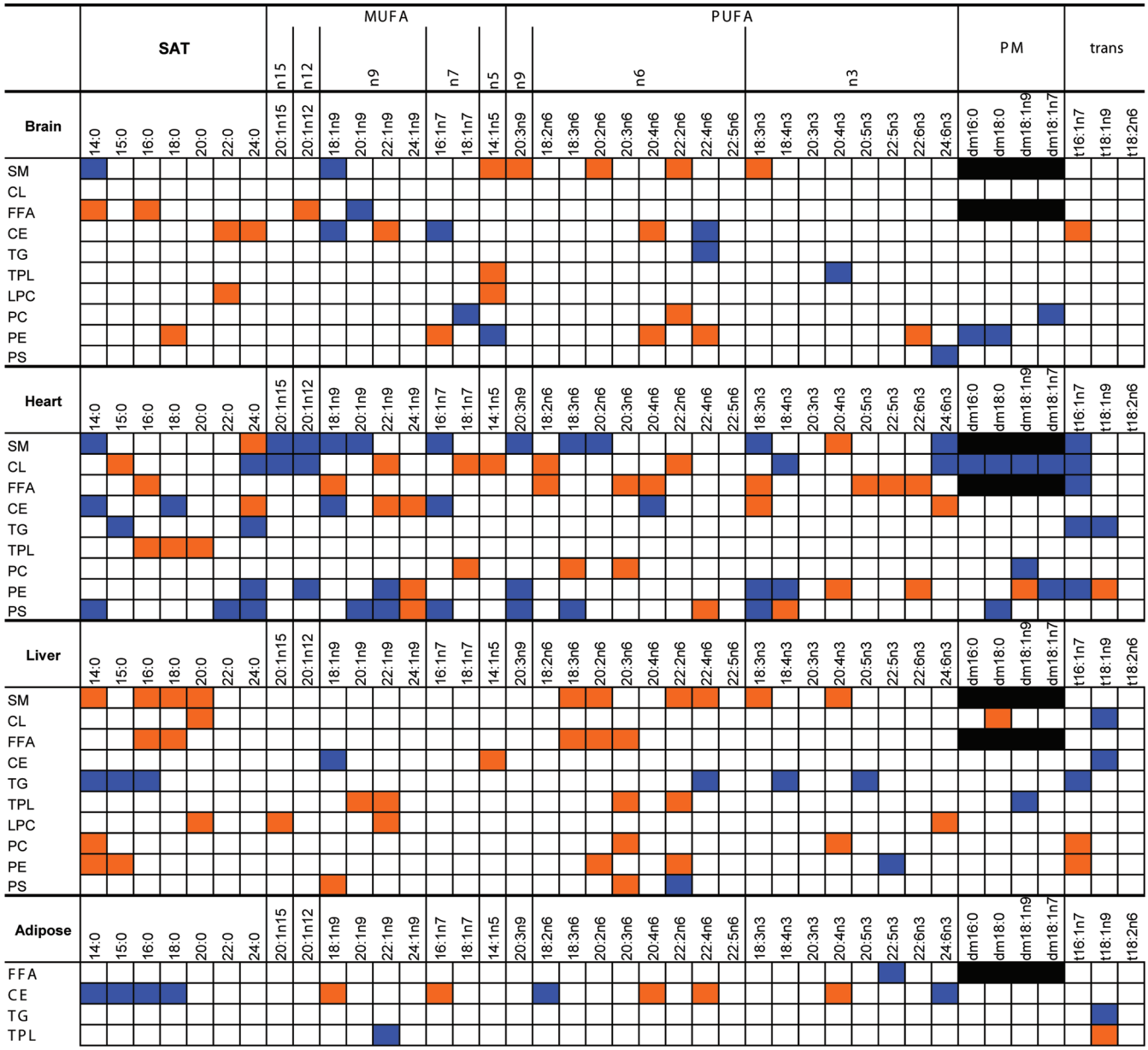

Figure 2. Complete heat map representation of changes in lipid levels following pyridine treatment in brain, heart, liver, and adipose. Significant changes as determined by a two-tailed Student's t test ($p < 0.05$) are indicated graphically such that blue = decreases, orange = increases, white = no change, and black = lipid not naturally present. Lipid subclasses are divided into SAT, MUFAs, polyunsaturated fatty acids (PUFAs), terminal double bond locations in relation to the ω terminus (ωX = nX), PM, and *trans*-fatty acids (trans). Lipid class abbreviations are as follows (for those not previously defined): SM, sphingomyelin; CL, cardiolipin; FFA, free fatty acids; TG, triglycerides; TPL, total phospholipids; LPC, lyso-phosphatidylcholine; PC, phosphatidylcholine; PE, phosphatidylethanolamine; and PS, phosphatidylserine/inositol. Individual fatty acid nomenclature follows standard naming conventions (e.g., 14:0 for tetradecanoic or myristic acid). See Table S5 for a full list of all scientific names, molecular names and common names.

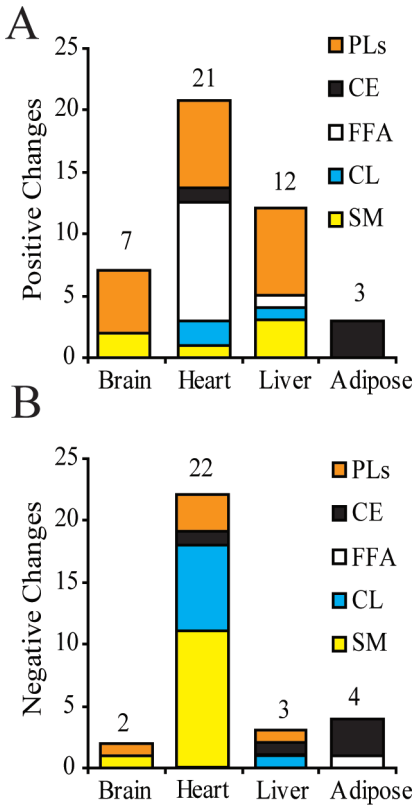

Figure 3. Number of significant positive (A) and negative (B) tissue lipid concentration changes detected in pyridine-treated animals by PLS analysis. The total number of changes within each tissue is displayed above each stacked bar. The heart showed the greatest number of changes (~60% of observed) and, like the liver, showed changes in each of the six major lipid classes shown here: SM, CL, FFAs, phospholipids (PLs), CE, and TGs. For simplicity, all phospholipids were grouped in this figure. FDR correction of two-tailed *t* tests using $q = 0.1$ identified a similar set of variables (Figure S1). Changes in specific residues are listed in Table S6.

CEs, and SM levels (Figures 2 and 3 and Table 1), while subtle shifts in FFAs were also observed. Although changes in TPL levels were not detected (Table 1), alterations were seen in the PC and PE subclasses. The total abundance of PC declined 1.1-fold or 10% (control, 47100 ± 3700; treated, 41600 ± 2500 nmol/g) in this tissue. At the lipid class level, changes were not definitive with only suggestions of SAT ($p = 0.07$) and MUFA ($p = 0.06$) declines but no effects upon PUFA concentrations ($p = 0.2$). While changes in total brain PE levels were not observed (control, 32700 ± 8100; treated, 33700 ± 2700 nmol/g), this lipid class was remodeled with increases in SATs and PUFAs but not MUFAs (Table 1). Results showed increases in SAT (control, 9200 ± 1200; treated, 11400 ± 700 nmol/g), PUFA (control, 2000 ± 800; treated, 16000 ± 1400 nmol/g), n3 (control, 7700 ± 700; treated, 10500 ± 1300 nmol/g), and n6 (control, 4200 ± 400; treated, 5400 ± 400 nmol/g) lipid classes, with increases in both PE-associated arachidonic acid (AA; control, 3459 ± 405; treated, 4593 ± 341nmol/g) and docosahexaneoic acid (DHA; control, 22:6n3, 7500 ± 700; treated, 10200 ± 1300 nmol/g). The brain PE fraction also displayed decreases in total PMs (control, 5300 ± 2700; treated, 1900 ± 400 nmol/g), as did the PC fraction (control, 7.3 ± 4.3; treated, 0.9 ± 1.8 nmol/g); however, the PC fraction contained a single species, 1-enyl-1,11-octadecadienoic acid (dm18:1n7).

Stable concentrations (control, 377 ± 82; treated, 393 ± 16 nmol/g) of free stearic acid (18:0) in the brain hid changes in other free SATs when displayed as a class (Table 1). However, increases were observed in brain myristic acid (14:0; control, 64 ± 13; treated, 86 ± 5.6 nmol/g), palmitic acid (16:0; control, 400 ± 40; treated, 520 ± 15 nmol/g), and 8-eicosaenoic acid (20:1n12; control, 13 ± 1.0; treated, 16 ± 1.3 nmol/g), and a decrease was observed in eicosenoic acid (20:1n9; control, 7.2 ± 1.0; treated, 4.7 ± 1.1).

CEs showed decreases in MUFAs (control: 1,140 ± 140; treated: 760 ± 80 nmol/g), including both n7 (control, 120 ± 10; treated, 91 ± 6 nmol/g) and n9 (control, 970 ± 110; treated, 630 ± 80 nmol/g) but an increase in *trans*-fatty acids (control, 69 ± 23; treated, 140 ± 15 nmol/g) due to changes in 9-*trans*-hexadecenoic acid (*trans*-16:1n7). Decreases in n9 were due mainly to a drop in oleic acid (18:1n9; control, 930 ± 110; treated, 560 ± 65 nmol/g). While significant changes in CE-associated PUFAs were not observed, AA increased in pyridine-treated mice (control, 9.7 ± 1.5; treated, 23 ± 4.5 nmol/g).

Although the brain SM SAT levels were not altered (Table 1), the MUFAs in these tissue lipids decreased 1.4-fold (control, 630 ± 100; treated, 470 ± 90 nmol/g), while PUFAs increased 1.6-fold (control, 240 ± 70; treated, 390 ± 40 nmol/g), with equivalent relative increases in both n3 (control, 60 ± 20; treated, 90 ± 20 nmol/g) and n6 fatty acids (control, 170 ± 50; treated, 280 ± 30 nmol/g). MUFA declines were limited to products of the δ-9 desaturase stearoyl CoA desaturase, decreasing (control, 490 ± 100; treated, 200 ± 40 nmol/g; Table 1).

Pyridine treatment also produced effects on a number of other stearoyl CoA desaturase-dependent metabolites. These included decreases in CE-associated 16:1n7 (control, 54 ± 8; treated, 36 ± 5 nmol/g) and 18:1n9 (control, 930 ± 110; treated, 570 ± 70 nmol/g) as well as increases in 13-docosenoic acid (22:1n9; control, 7.1 ± 5.1; treated, 23 ± 7 nmol/g), decreases in FFA-associated 20:1n9 (control, 7.2 ± 1.0; treated, 4.7 ± 1.1 nmol/g), decreases in SM-associated 18:1n9 (control, 305 ± 58; treated, 95 ± 16 nmol/g), and increases in SM-associated 9-tetradecenoic acid (14:1n5; control, 72 ± 26; treated, 180 ± 24 nmol/g) and 5,8,11-eicosatrienoic acid (20:3n9; control, 8.1 ± 4; treated, 18 ± 2 nmol/g).

Heart Lipid Metabolism. The heart displayed the most diverse response of the four tissues examined (Figure 2), with significant effects in phospholipids, FFAs, CEs, SMs, and CL (Table 1). The TGs had few responses at a significance level of $p < 0.05$ (Figure 2) only showing a decrease in *trans*-fatty acids (control, 104 ± 22; treated, 56 ± 30 nmol/g), and these were excluded after FDR adjustments (Figure S1 and Table S6).

With respect to phospholipids (Table 1), SATs (control, 20100 ± 2000; treated, 23900 ± 2000 nmol/g) and n7 MUFAs (control, 1510 ± 100; treated, 1720 ± 100) showed significant changes, while alterations in TPL were not definitive ($p = 0.06$; control, 29100 ± 3000; treated, 33700 ± 3000 nmol/g). When inspected as independent classes, PE showed significant enrichment in n3 PUFAs (control, 5930 ± 1200; treated, 7970 ± 600 nmol/g), which were ~95% DHA in both cases, as well as elevated *trans*-fatty acids (control, 33 ± 9.4; treated, 53 ± 3.8 nmol/g). In contrast, the changes in total PE molar abundance were not definitive ($p = 0.06$; control, 7360 ± 1300; treated, 8990 ± 600 nmol/g). Few changes were observed in PC.

The cardiac FFAs were elevated 30–60% including total fatty acids (control, 80 ± 67; treated, 1350 ± 150 nmol/g), SATs (control, 440 ± 60; treated, 580 ± 85 nmol/g), MUFAs (control, 240 ± 12; treated, 300 ± 30 nmol/g), PUFAs (control, 290 ± 28; treated, 470 ± 36 nmol/g), n3 (control, 51 ± 11; treated, 110 ± 3.5 nmol/g), n6 (control, 240 ± 22; treated, 350 ± 32 nmol/g), and n9 (control, 200 ± 12; treated, 250 ± 23 nmol/g).

Table 1. Fold-Changes in Lipid Subclass Component Molar Abundance Produced by i.p. Pyridine[a]

	total FA	SAT	MUFA	n7	n9	PUFA	n3	n6	PM	trans
					brain					
SM			−1.4 ± 0.2		**−2.5 ± 0.4**	**1.6 ± 0.1**	1.6 ± 0.3	**1.6 ± 0.2**	NA	
CL										
FFA									NA	
CE			**−1.5 ± 0.2**	−1.3 ± 0.1	**−1.6 ± 0.2**					**2.1 ± 0.2**
TG										
TPL										
PC	−1.1 ± 0.1									
PE		1.2 ± 0.1				**1.3 ± 0.1**	1.4 ± 0.2	**1.3 ± 0.1**	−2.9 ± 0.6	
PS										
					heart					
SM			**−1.5 ± 0.3**	**−2.2 ± 0.4**	**−1.5 ± 0.3**				NA	**−6.8 ± 2.7**
CL				1.4 ± 0.2				1.3 ± 0.1	**−3.8 ± 1.5**	−1.9 ± 0.8
FFA	1.4 ± 0.2	1.3 ± 0.2	1.3 ± 0.1		**1.3 ± 0.1**	**1.6 ± 0.1**	**2.2 ± 0.1**	**1.5 ± 0.1**	NA	
CE	−1.2 ± 0.1				**−1.4 ± 0.1**			−1.3 ± 0.2		
TG										−2.3 ± 1.4
TPL		1.2 ± 0.1		1.1 ± 0.1						
PC										
PE	1.2 ± 0.1					**1.3 ± 0.1**	**1.3 ± 0.1**			1.2 ± 0.1
PS					−1.6 ± 0.5					
					liver					
SM	1.5 ± 0.3	1.5 ± 0.3		**1.6 ± 0.2**		1.6 ± 0.2	1.7 ± 0.3	**1.6 ± 0.3**	NA	
CL										
FFA		**1.3 ± 0.1**							NA	
CE			**−1.5 ± 0.2**		**−1.9 ± 0.3**		−1.4 ± 0.2			
TG		**−1.4 ± 0.2**								−1.4 ± 0.2
TPL										
PC										1.4 ± 0.2
PE										
PS										
					adipose					
FFA									NA	
CE		**−2.1 ± 0.5**	1.8 ± 0.5	**2.3 ± 0.7**			1.6 ± 0.4			
TPL										
TG										

[a] Note that values are means ± SD fold changes between pyridine- ($n = 4$) and vehicle-treated ($n = 5$) groups (bold font, $p < 0.01$; all others, $p < 0.05$; two-tailed t test). A blank cell indicates no change; ND, not detected; NA, not analyzed; nX = ωX where X indicates the terminal double bond carbon relative to the ω terminal.

The total level of CEs decreased (control, 710 ± 65; treated, 600 ± 65 nmol/g), as did both the n6 (control, 170 ± 24; treated, 130 ± 20 nmol/g) and n9 (control, 110 ± 10; treated, 74 ± 3.9 nmol/g) esters. Decreases in SM levels were observed in MUFA (control, 200 ± 20; treated, 130 ± 20 nmol/g), n7, n9, and *trans*-fatty acids. CL displayed declines in PM (control, 140 ± 40; treated, 37 ± 19 nmol/g) and *trans*-fatty acids (control, 29 ± 7.2; treated, 17 ± 6.7 nmol/g) but increases in n6 (control, 3540 ± 560; treated, 4460 ± 270 nmol/g) and n7 (control, 540 ± 84; treated, 740 ± 120 nmol/g) as shown in Table 1.

Liver Lipid Metabolism. In the liver, pyridine exposure showed subtle effects on FFAs, CEs, and SM levels as shown in Figure 3 and Table 1. While hepatic TGs showed changes with $p < 0.05$ (Figure 2), the significance of these findings did not appear in the PLS analysis (Figure 1) and did not survive the FDR adjustments (Figure S1). However, the liver TGs exhibited decreases in SATs (control, 5500 ± 670; treated, 3900 ± 420 nmol/g) and t16:1n7 (control, 240 ± 40; treated, 170 ± 27 nmol/g), while the FFAs were enriched in SATs (control, 700 ± 90; treated, 920 ± 80 nmol/g). The total concentration of SM increased (control, 1260 ± 150; treated, 1860 ± 320 nmol/g), as did SM SATs (control, 800 ± 100; treated, 1240 ± 250 nmol/g) and PUFAs (control, 130 ± 30; treated, 210 ± 30 nmol/g).

Few effects were observed in PM levels, with only an increase in CL-associated 1-enyl-octadecenoic acid (dm18:0) and a decrease in TPL-associated 1-enyl-1,9-octadecadienoic acid (dm18:1n9). TG-associated 1-enyl-hexadecenoic acid (dm16:0) exhibited an increase; however, one of the animals did not have measurable dm16:0 levels, subsequently giving a p value of 0.06 (Table S3).

Adipose Lipid Metabolism. In the adipose tissue, the CEs were the only lipid class significantly affected by pyridine exposure (Figure 2 and Table 1), even though the free concentration of 22:5n3 did decrease (Table S6). While the total CE mass did not change, its composition shifted toward unsaturated species with an overall decrease in SATs (control, 3100 ± 550; treated, 1550 ± 350 nmol/g) and increases in MUFAs (control, 1400 ± 390; treated, 2540 ± 760 nmol/g), n3 (control, 230 ± 40; treated, 350 ± 90 nmol/g), and n7 (control, 150 ± 30; treated, 340 ± 110 nmol/g).

Discussion

Pyridine is a compound with low acute toxicity that produces subtle deleterious effects, such as mild symptoms of central nervous system injury (headache, dizziness, insomnia, nausea, and anorexia), suggesting that organ-specific oxidative stress and membrane damage may occur following exposure (*1, 17*). We hypothesized that cellular lipids may be altered by pyridine exposure, due to their responsiveness to oxidative stress coupled with the reported pyridine-dependent induction of CYP 2E1 (*5, 7*) and this enzyme's propensity to liberate intercellular ROS (*9*). This hypothesis was tested by targeted analysis of an array of structural lipids in multiple tissues of pyridine-exposed mice.

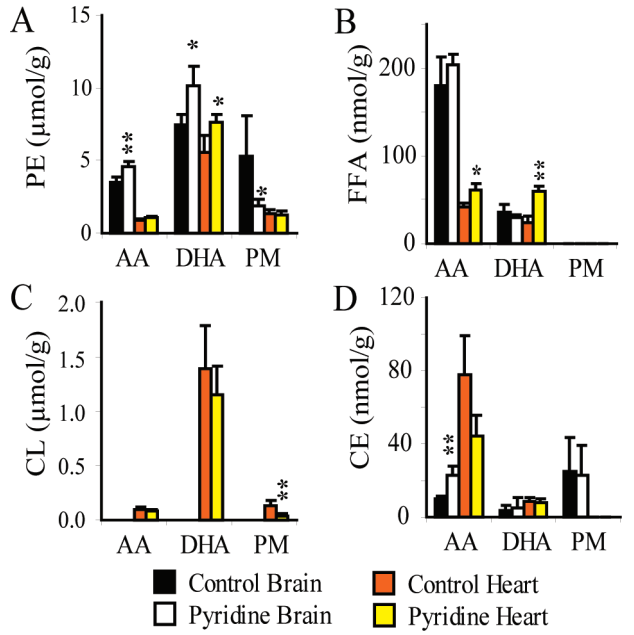

Figure 4. Pyridine treatment affects long-chain PUFA concentrations on a tissue-specific basis. The levels of brain and heart AA (20:4n6), docosahexaenoic acid (DHA; 22:6n3), and PM are shown for PEs (A), FFAs (B), CLs (C), and CEs (D). Concentrations are reported as the mean ± standard deviation for control ($n = 5$) and pyridine-treated ($n = 4$) groups, with statistical significance examined using a two-tailed t test (* = $p < 0.05$, and ** = $p < 0.01$). Significant changes were not observed for AA, DHA, or PM in any of the lipid subclasses not shown here.

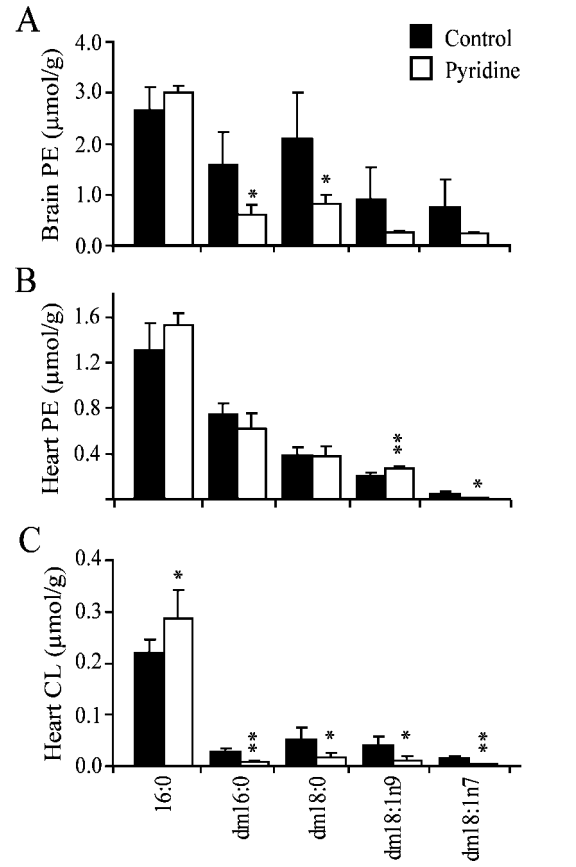

Figure 5. Dimethyl acetal (dm) speciation in brain (A) and heart (B) PE and in heart (C) CL. The concentration of palmitate (16:0) is shown to provide an indication of the relative abundance of ester and ether-linked lipids for each of the displayed lipid classes. The sum of the dm species constitutes the PM fractions. The variance in the control brain PE was due to a single high sample. Results are the mean ± standard deviation with significant differences between control ($n = 5$) and pyridine treatment ($n = 4$) being indicated at the $p < 0.05$ (*) and $p < 0.01$ (**) levels.

During the course of this study, a number of tissue and lipid class-specific alterations were revealed that clearly discriminated pyridine-treated and control animals (Figures 1 and 3 and Table S6). Statistical analysis by PLS and FDR-adjusted p values identified 60 distinct lipids whose levels were significantly altered by exposure to pyridine. One of the challenges in this type of study is interpreting the biological significance of the observed fluctuations. Accordingly, shifts in lipid levels that address the main hypothesis are highlighted in the following discussion; however, it is probable that other important observations could be mined from the data set in Table S6.

Pyridine exposure produced significant effects in the PMs and phospholipids of the brain and heart but not the liver or adipose. In both affected tissues, PE was the most dramatically altered phospholipid, with both PLS and FDR-adjusted p values identifying four and eight lipids, respectively, whose levels altered following pyridine treatment (Table S6). In the brain, phospholipid pools were depleted in PE-associated PMs, while enriched in PE-associated stearate (18:0), palmitoleate (16:1n7), AA, and DHA, indicating extensive remodeling. In contrast, changes in heart phospholipids were relegated to enrichment in PE long-chain PUFAs, while CL isolates showed a dramatic depletion in PMs (Figure 4).

PMs make up ~18% of the phospholipid mass in humans, with PE containing the highest proportion of tissue PMs, reaching 70% in some tissues (*26*). In addition, PMs are oxidant-sensitive components of lipid rafts (*26*), membrane microdomains involved in signal transduction (*27*). The unique vinyl-ether structure of the PMs (i.e., an ether-linked *sn*-1 alkyl chain α to a *cis*-olefin) is believed to account for their unique sensitivity to ROS (*26, 28*). This oxidant sensitivity has prompted the hypothesis that PMs act as ROS scavengers, protecting other membrane lipids and proteins from oxidative damage (*29*), and there is strong evidence that oxidative stress can lead to the phospholipase-dependent depletion of membrane PMs (*30*). Notably, reduced cellular PMs occur in various degenerative diseases (*27*), especially conditions with elevated oxidative stress such as peroxisomal disorders and Alzheimer's disease (*31, 32*). An earlier study indicated elevated oxidative stress in the brains of mice after 3 months of pyridine exposure (*15*). Our observation of reduced brain PE PMs is consistent with the occurrence of oxidative stress in the mouse brain after as little as 1 week of pyridine exposure.

As mentioned above, the changes in cardiac PM were limited to effects on plasmenyl-CL, as opposed to the effects on plasmenyl-PE observed in the brain. While plasmenyl-CLs have been previously reported (*33*), the biological role of this lipid class is unknown. As a class, CLs are tetrasubstituted phospholipids found almost entirely in membranes containing respiratory chain transport complexes (*34*). Mammalian CL contains up to 90 mol% of 18:2n6, that is, linoleic acid (*35*). Decreases in CL-associated PM in the heart were reflected in a concomitant increase in 18:2n6, suggesting replenishment of plasmenyl-CL with the more abundant acylated form. It is particularly interesting that these changes in CL PM were distinct from those found in PE from the same extracts (Figure 5). Therefore, assuming that the oxidant scavenging role of PM is conserved within CL, the decline in plasmenyl-CL would argue for elevation in mitochondrial ROS generation. Such an oxidative environment would occur within mitochondria, exhibiting enhanced rates of long-chain fatty acid combustion (*36*). The dramatic elevation in FFAs in the heart of the pyridine-exposed

animals (Table 1) is intriguing in the face of this hypothesis. A total of eight FFAs increased significantly as identified by both PLS and FDR-adjusted p value analyses. With the exception of increased saturates in the liver, elevated fatty acid levels were not observed in other tissues. The elevation in the cardiac FFAs pool could result from multiple events including an increased availability/uptake of plasma lipids (*37*), an increased liberation from intracellular stores, a reduction in cellular β-oxidation, or an enhanced depuration of these lipids into the interstitial space (*38*). While further exploration of this finding was beyond the scope of this study, the depletion of plasmenyl-CL suggests that future studies should assess carnatine palmitoyl transferase activity in the hearts of pyridine-exposed animals.

As opposed to the changes described in the brain and heart, the most striking effect on lipids in the liver was a 50% increase in the total concentration of SM, as well as in each of its lipid subclasses except the n9-MUFAs. Interestingly, decreases were observed in the SM n9-MUFA fraction in both the heart and the brain. SM is a component of membranes lipid rafts (*39*) and chromatin-associated intranuclear lipid (*40*). Elevations in hepatic canalicular membrane SM have been reported after exposure to diosgenin, an inducer of bile salt excretion, which protected the liver from toxic doses of taurocholate (*41*). In addition, CYP 2E1 expression in the liver is positively correlated with hepatic steatosis (*42*). Therefore, enrichment in hepatic SM in the current pyridine exposure study is consistent with a compensatory mechanism, stabilizing canalicular membranes and mitigating the pro-steatotic effects expected with a pyridine-associated CYP 2E1 induction.

The only lipid class showing changes in all analyzed tissues were the CEs; however, the degree of change was tissue-specific. In the current study, the total concentration of CEs was only affected in the heart, where they declined 20%. This decrease could be related to the apparent increased metabolic demand for long-chain fatty acids for mitochondrial respiration, which would support the hypothesis of increased mitochondrial stress. However, the heart showed a selective loss in n9-MUFAs and n6-PUFAs acylation, rather than an equivalent loss in all acyl types, as seen in the FFA fraction. A selective loss of MUFAs was also observed in the brain and liver. In fact, products of the stearoyl Co-A desaturase (e.g., 18:1n9) decreased in brain, heart, and liver. In contrast, the adipose tissue showed a ~2-fold increase in these monounsaturated CEs, while the saturated CEs decreased. Interestingly, chronic low doses of pyridine have been reported to influence cholesterol metabolism in female rats (*3*). Together, these data suggest that pyridine exposure can impact cholesterol trafficking.

The data presented here indicate a complex, but tissue-specific, impact of pyridine exposure on lipid metabolism, a component of which is linked to oxidative stress. However, the exact mechanism(s) responsible for the observed effects will require careful exploration. For example, pyridine inhalation also induces nasal carboxylesterase activity (*43*), an enzyme class that may also have roles in lipid metabolism (*44*). Given the broad nature of the observed changes in tissue lipids, an encompassing explanation for these responses would be satisfying; however, such speculation is risky. The most explicable findings are those consistent with a tissue-specific response to oxidative stress including a CYP 2E1-induced stimulation of ROS (*45–47*). Moreover, previous reports suggest that the responses of brain and liver differ from those of the heart following exposure to model CYP 2E1 inducers (*47*). While changes in the brain and liver lipids differed, components of their underlying response may have been similar. In the brain, PE PMs provide endogenous protection to oxidative challenges (*48*). In the liver, such a role has not been reported; however, the high rate of phospholipid biosynthesis in this tissue could mask such an effect. The heart only revealed subtle changes in PE PMs, while PMs within the CL showed a similar broad decline, suggesting a mitochondrial stress in this tissue. To further the understanding of these results, future experiments should be conducted to segregate the cardiac-specific effects between enhanced cardiac fatty acid combustion and other specific sources of oxidant damage. To definitively implicate CYP 2E1 in these responses, it would be particularly interesting to evaluate the effect of pyridine intoxication on the cardiac lipids of the CYP 2E1-null mouse. Moreover, greater mechanistic understanding could be achieved by comparing our present findings to the responses of the Swiss Webster mouse to other known CYP 2E1 inducers (e.g., ethanol) and cardiotoxicants such as doxorubicin (*49*). In addition, future studies should measure levels and/or activity of CYP 2E1, as well as other enzymes of interest such as stearoyl-CoA desaturase, to verify the effects of treatment upon enzyme levels.

In summary, our findings support the hypothesis that PMs can serve as antioxidants in the brain and possibly cardiac mitochondria, and the observed changes in hepatic SMs are consistent with a protective response to hepatic oxidative stress. The consequences of pyridine-induced changes in cardiac FFA and systemic cholesterol metabolism are complex and deserve additional attention.

Acknowledgment. We thank Raymond Wan and Hiroshi Mamitsuka for many useful discussions. C.E.W. was supported by a Japanese Society for the Promotion of Science (JSPS) postdoctoral fellowship and an EU Sixth Framework Programme (FP6) Marie Curie International Incoming Fellowship (IIF). This work was supported in part by NIEHS Grant R37 ES02710 and NIEHS Superfund Grant P42 ES04699. Support for J.W.N. was provided by the U.S. Department of Agriculture, ARS Project 5306-51530-016-00D, during the writing phase of this manuscript. We thank Alan Buckpitt, Dexter Morin, Ryan Davis, David Lawson, and C. J. Dillard for technical assistance. We also thank Thuan Nquyen of the UC Davis Department of Statistics for an independent evaluation of the data treatments applied in this manuscript.

Supporting Information Available: Excel file with quantitative values (nmol/g tissue) of all lipids measured in this study (Tables S1−S4); a table with the scientific name, molecular name, and common name of all fatty acids reported (Table S5); a list of the significant variables identified with PLS vs Student's t test and FDR analyses (Table S6); a list of the variables excluded from the PLS analysis due to nondetected values (Table S7); and the number of significant positive and negative tissue lipid concentration changes detected in pyridine-treated animals after applying a FDR correction to the t test results (Figure S1). This information is available free of charge via the Internet at http://pubs.acs.org.

References

(1) ATDSR (1992) Toxicological Profile for Pyridine, U.S. Department of Health and Human Services, Public Health Service, Agency for Toxic Substances and Disease Registry, Atlanta, GA.
(2) Ji, L., Melkonian, G., Riveles, K., and Talbot, P. (2002) Identification of pyridine compounds in cigarette smoke solution that inhibit growth of the chick chorioallantoic membrane. *Toxicol. Sci. 69*, 217–225.
(3) NTP (2000) National Toxicology Program Technical Report on the Toxicology and Carcinogenesis Studies of Pyridine (CAS No. 110-86-1) in F344/N Rats, Wistar Rats, and B6C3F1 Mice (Drinking Water Studies),

U.S. Department of Health and Human Services, Public Health Service, National Institutes of Health, Research Triangle Park, NC.
(4) Venkatakrishna-Bhatt, H., Shah, M. P., and Kashyap, S. K. (1975) Toxicological effects of intravenous administration of pyridine in anaesthetized dogs. *Toxicology 4*, 165–169.
(5) Kim, S. G., Williams, D. E., Schuetz, E. G., Guzelian, P. S., and Novak, R. F. (1988) Pyridine induction of cytochrome P-450 in the rat: Role of P-450j (alcohol-inducible form) in pyridine N-oxidation. *J. Pharmacol. Exp. Ther. 246*, 1175–1182.
(6) Kim, H., Putt, D. A., Zangar, R. C., Wolf, C. R., Guengerich, F. P., Edwards, R. J., Hollenberg, P. F., and Novak, R. F. (2001) Differential induction of rat hepatic cytochromes P450 3A1, 3A2, 2B1, 2B2, and 2E1 in response to pyridine treatment. *Drug Metab. Dispos. 29*, 353–360.
(7) Page, D. A., and Carlson, G. P. (1994) The effect of pyridine on the in vitro and in vivo metabolism of ethyl carbamate (urethane) by rat and mouse. *Carcinogenesis 15*, 2177–2181.
(8) Leclercq, I., Horsmans, Y., Desager, J. P., Pauwels, S., and Geubel, A. P. (1999) Dietary restriction of energy and sugar results in a reduction in human cytochrome P450 2E1 activity. *Br. J. Nutr. 82*, 257–262.
(9) Song, B. J., Gelboin, H. V., Park, S. S., Yang, C. S., and Gonzalez, F. J. (1986) Complementary DNA and protein sequences of ethanol-inducible rat and human cytochrome P-450s. Transcriptional and post-transcriptional regulation of the rat enzyme. *J. Biol. Chem. 261*, 16689–16697.
(10) Nieto, N., Friedman, S. L., and Cederbaum, A. I. (2002) Stimulation and proliferation of primary rat hepatic stellate cells by cytochrome P450 2E1-derived reactive oxygen species. *Hepatology 35*, 62–73.
(11) Ekstrom, G., and Ingelman-Sundberg, M. (1989) Rat liver microsomal NADPH-supported oxidase activity and lipid peroxidation dependent on ethanol-inducible cytochrome P-450 (P-450IIE1). *Biochem. Pharmacol. 38*, 1313–1319.
(12) Vaz, A. D., Roberts, E. S., and Coon, M. J. (1990) Reductive beta-scission of the hydroperoxides of fatty acids and xenobiotics: Role of alcohol-inducible cytochrome P-450. *Proc. Natl. Acad. Sci. U.S.A. 87*, 5499–5503.
(13) Lieber, C. S. (1997) Cytochrome P-4502E1: Its physiological and pathological role. *Physiol. Rev. 77*, 517–544.
(14) Nieto, N., Greenwel, P., Friedman, S. L., Zhang, F., Dannenberg, A. J., and Cederbaum, A. I. (2000) Ethanol and arachidonic acid increase alpha 2(I) collagen expression in rat hepatic stellate cells overexpressing cytochrome P450 2E1. Role of H_2O_2 and cyclooxygenase-2. *J. Biol. Chem. 275*, 20136–20145.
(15) Pinsky, C., and Bose, R. (1988) Pyridine and other coal tar constituents as free radical-generating environmental neurotoxicants. *Mol. Cell. Biochem. 84*, 217–222.
(16) Kim, S. G., Shehin, S. E., States, J. C., and Novak, R. F. (1990) Evidence for increased translational efficiency in the induction of P450IIE1 by solvents: Analysis of P450IIE1 mRNA polyribosomal distribution. *Biochem. Biophys. Res. Commun. 172*, 767–774.
(17) Jori, A., Calamari, D., Cattabeni, F., Di Domenico, A., Galli, C. L., Galli, E., and Silano, V. (1983) Ecotoxicological profile of pyridine. Working party on ecotoxicological profiles of chemicals. *Ecotoxicol. Environ. Saf. 7*, 251–275.
(18) Wheelock, C. E., Goto, S., Hammock, B. D., and Newman, J. W. (2007) Clofibrate-induced changes in the liver, heart, brain and white adipose lipid metabolome of Swiss-Webster mice. *Metabolomics 3*, 137–145.
(19) Watkins, S. M., Reifsnyder, P. R., Pan, H. J., German, J. B., and Leiter, E. H. (2002) Lipid metabolome-wide effects of the PPARgamma agonist rosiglitazone. *J. Lipid Res. 43*, 1809–1817.
(20) Mutch, D. M., Grigorov, M., Berger, A., Fay, L. B., Roberts, M. A., Watkins, S. M., Williamson, G., and German, J. B. (2005) An integrative metabolism approach identifies stearoyl-CoA desaturase as a target for an arachidonate-enriched diet. *FASEB J. 19*, 599–601.
(21) Hammond, L. E., Albright, C. D., He, L., Rusyn, I., Watkins, S. M., Doughman, S. D., Lemasters, J. J., and Coleman, R. A. (2007) Increased oxidative stress is associated with balanced increases in hepatocyte apoptosis and proliferation in glycerol-3-phosphate acyltransferase-1 deficient mice. *Exp. Mol. Pathol. 82*, 210–219.
(22) Ruiz, J. I., and Ochoa, B. (1997) Quantification in the subnanomolar range of phospholipids and neutral lipids by monodimensional thin-layer chromatography and image analysis. *J. Lipid Res. 38*, 1482–1489.
(23) Benjamini, Y., and Hochberg, Y. (1995) Controlling the false discovery rate: A practical and powerful approach to multiple testing. *J. R. Stats. Soc. Ser. B (Methodological) 57*, 289–300.
(24) Geladi, P., and Kowalski, B. R. (1986) Partial least-squares regression: A tutorial. *Anal. Chim. Acta 185*, 1–17.
(25) Martens, H., and Martens, M. (2000) Modified Jack-knife estimation of parameter uncertainty in bilinear modelling by partial least squares regression (PLSR). *Food Qual. Pref. 11*, 5–16.
(26) Nagan, N., and Zoeller, R. A. (2001) Plasmalogens: biosynthesis and functions. *Prog. Lipid Res. 40*, 199–229.
(27) Brites, P., Waterham, H. R., and Wanders, R. J. (2004) Functions and biosynthesis of plasmalogens in health and disease. *Biochim. Biophys. Acta 1636*, 219–231.
(28) Zoeller, R. A., Lake, A. C., Nagan, N., Gaposchkin, D. P., Legner, M. A., and Lieberthal, W. (1999) Plasmalogens as endogenous antioxidants: Somatic cell mutants reveal the importance of the vinyl ether. *Biochem. J. 338*, 769–776.
(29) Reiss, D., Beyer, K., and Engelmann, B. (1997) Delayed oxidative degradation of polyunsaturated diacyl phospholipids in the presence of plasmalogen phospholipids in vitro. *Biochem. J. 323*, 807–814.
(30) McHowat, J., Liu, S., and Creer, M. H. (1998) Selective hydrolysis of plasmalogen phospholipids by Ca2+-independent PLA2 in hypoxic ventricular myocytes. *Am. J. Physiol. 274*, C1727–1737.
(31) Moreira, P. I., Honda, K., Zhu, X., Nunomura, A., Casadesus, G., Smith, M. A., and Perry, G. (2006) Brain and brawn: Parallels in oxidative strength. *Neurology 66*, S97–S101.
(32) Ferdinandusse, S., Finckh, B., de Hingh, Y. C., Stroomer, L. E., Denis, S., Kohlschutter, A., and Wanders, R. J. (2003) Evidence for increased oxidative stress in peroxisomal D-bifunctional protein deficiency. *Mol. Genet. Metab. 79*, 281–287.
(33) Schlame, M., Rua, D., and Greenberg, M. L. (2000) The biosynthesis and functional role of cardiolipin. *Prog. Lipid Res. 39*, 257–288.
(34) Gohil, V. M., Hayes, P., Matsuyama, S., Schagger, H., Schlame, M., and Greenberg, M. L. (2004) Cardiolipin biosynthesis and mitochondrial respiratory chain function are interdependent. *J. Biol. Chem. 279*, 42612–42618.
(35) Schlame, M., Ren, M., Xu, Y., Greenberg, M. L., and Haller, I. (2005) Molecular symmetry in mitochondrial cardiolipins. *Chem. Phys. Lipids 138*, 38–49.
(36) Yamagishi, S. I., Edelstein, D., Du, X. L., Kaneda, Y., Guzman, M., and Brownlee, M. (2001) Leptin induces mitochondrial superoxide production and monocyte chemoattractant protein-1 expression in aortic endothelial cells by increasing fatty acid oxidation via protein kinase A. *J. Biol. Chem. 276*, 25096–25100.
(37) Teusink, B., Voshol, P. J., Dahlmans, V. E., Rensen, P. C., Pijl, H., Romijn, J. A., and Havekes, L. M. (2003) Contribution of fatty acids released from lipolysis of plasma triglycerides to total plasma fatty acid flux and tissue-specific fatty acid uptake. *Diabetes 52*, 614–620.
(38) Julien, P., Dagenais, G. R., Gailis, L., and Roy, P. E. (1978) Role of cardiac lymph and interstitial fluid in lipid metabolism of canine heart. *Can. J. Physiol. Pharmacol. 56*, 1041–1046.
(39) Filippov, A., Oradd, G., and Lindblom, G. (2005) Sphingomyelin structure influences the lateral diffusion and raft formation in lipid bilayers. *Biophys. J. 90*, 2086–2092.
(40) Albi, E., and Viola Magni, M. P. (2004) The role of intranuclear lipids. *Biol. Cell. 96*, 657–667.
(41) Amigo, L., Mendoza, H., Zanlungo, S., Miquel, J. F., Rigotti, A., Gonzalez, S., and Nervi, F. (1999) Enrichment of canalicular membrane with cholesterol and sphingomyelin prevents bile salt-induced hepatic damage. *J. Lipid Res. 40*, 533–542.
(42) Orellana, M., Rodrigo, R., Varela, N., Araya, J., Poniachik, J., Csendes, A., Smok, G., and Videla, L. A. (2005) Relationship between in vivo chlorzoxazone hydroxylation, hepatic cytochrome P450 2E1 content and liver injury in obese non-alcoholic fatty liver disease patients. *Hepatol. Res. 34*, 57–63.
(43) Nikula, K. J., Novak, R. F., Chang, I. Y., Dahl, A. R., Kracko, D. A., Zangar, R. C., Kim, S. G., and Lewis, J. L. (1995) Induction of nasal carboxylesterase in F344 rats following inhalation exposure to pyridine. *Drug Metab. Dispos. 23*, 529–535.
(44) Redinbo, M. R., and Potter, P. M. (2005) Mammalian carboxylesterases: from drug targets to protein therapeutics. *Drug Discovery Today 10*, 313–325.
(45) Klein, S. M., Cohen, G., Lieber, C. S., and Cederbaum, A. I. (1983) Increased microsomal oxidation of hydroxyl radical scavenging agents and ethanol after chronic consumption of ethanol. *Arch. Biochem. Biophys. 223*, 425–432.
(46) Reinke, L. A., Lai, E. K., DuBose, C. M., and McCay, P. B. (1987) Reactive free radical generation in vivo in heart and liver of ethanol-fed rats: Correlation with radical formation in vitro. *Proc. Natl. Acad. Sci. U.S.A. 84*, 9223–9227.
(47) Marin-Garcia, J., Ananthakrishnan, R., and Goldenthal, M. J. (1995) Heart mitochondria response to alcohol is different than brain and liver. *Alcohol.: Clin. Exp. Res. 19*, 1463–1466.
(48) Kuczynski, B., and Reo, N. V. (2006) Evidence that plasmalogen is protective against oxidative stress in the rat brain. *Neurochem. Res. 31*, 639–656.
(49) Combs, A. B., and Acosta, D. (1990) Toxic mechanisms of the heart: A review. *Toxicol. Pathol. 18*, 583–596.

TX7002454